Supporting Information File

Design of Need Based Phosphor and Scintillators by compositional modulation in $ZnGa_{2-x}Al_xO_4:Cr^{3+}$ Spinel: Pure Compound versus Solid Solutions

Santosh K. Gupta,[1,6*] Kathi Sudarshan[1,6#], P. Modak,[2,6]D. Chandrashekhar,[3]Mohit Tyagi,[4,6]Brindaban Modak,[5,6] M. Mohapatra,[1,6]

[1]*Radiochemistry Division, Bhabha Atomic Research Centre, Trombay, Mumbai-400085, India*
[2]*Radiological Safety Division,Atomic Energy Regulatory Board, Anushaktinagar, Mumbai-400094, India*
[3]*Product Development Division Bhabha Atomic Research Centre, Trombay, Mumbai-400085, India,*
[4]*Technical Physics Division,Bhabha Atomic Research Centre, Trombay, Mumbai-400085, India*
[5]*Chemistry Division,Bhabha Atomic Research Centre, Trombay, Mumbai-400085, India*
[6]*Homi Bhabha National Institute, Anushaktinagar, Mumbai – 400094, India*

S1. Materials and synthesis

All the samples of nominal composition as $Zn(Ga_{2-x}Al_x)O_4$ with 1.0 mol% Cr^{3+} doping was prepared using solid state method. The starting materials used were ZnO, Ga_2O_3, Al_2O_3 and Cr_2O_3. These oxides in stoichiometric proportions were well grounded using mortar and pestle. The samples were annealed in air at 900 °C for 15 hours. The temperature ramp was 10 deg per minute with waiting time of 30 minutes at 500 °C. The sample was allowed to cool to the room temperature, further grounded, and annealed again at 1200 °C for 15 hours. The temperature was raised at 10 °C per minute held for 30 minutes at 500 °C and 900 °C in the second annealing cycle.

S2. Characterization

Powder X-ray diffraction patterns of all the samples were acquired using a Proto make bench top AXRD machine using copper $k_\alpha$as X-ray source and in the angular range of 15 to 80 deg. The can rate was kept at 1.5 deg per minute. Total reflection X-ray Fluorescence (TXRF) measurements were carried out using an Atominstitut, Vienna, low Z – high Z TXRF spectrometer. Rh Kα monochromatic beam obtained from the Rh target X-ray tube was used in the present experiment. A few micrograms of the solid samples were dispersed in 500µL of 1% TRITON X-100 solution in a centrifuge tube and ~ 5 µL of this solution is pipette out and deposited on quartz sample supports. These sample supports were then taken for TXRF measurements.

Photoluminescence (PL) measurements were carried out using Edinburgh Instruments make F900 spectrometer with CD920 controller. A Xenon flash lamp of 150 W was used as excitation source. Excitation and emission spectra were recorded in steps of 1nm and a total of five scans

were taken for each excitation or emission scan for better statistics. For persistent luminescence (PerL) decay profiles, Edinburgh Instruments make F980 spectrometer with Xenon flash lamp was used.

Bruker make EMX series spectrometer was used for electron paramagnetic resonance (EPR) experiments. The spectrometer operated at X band (9.45 GHz) frequency with 2 Gauss modulation amplitude and 100 kHz modulation frequency. The paramagnetic signals were calibrated using DPPH as the field marker taking its g = 2.00036.

Positron annihilation lifetimes measurements were carried out a spectrometer having 265 ps resolution. Na-22 sandwiched between two identical polyimide films of 8 micron was used as source of positrons. The program PALSFit was used to resolve various positron lifetime components from the spectrum with appropriate corrections for the positrons annihilating in the source. These corrections were determined by analyzing positron annihilation spectrum from silicon as reference.Radio-luminescence was measured using an X-ray tube operated at 40kV and 10 mA. Theemission was recorded using an optical fiber and Avantes Spectrograph. The curve was correctedfor the spectral sensitivity of fiber and spectrograph.

S3. Computational details

All the DFT calculationshave been performed using Vienna ab initio simulation package (VASP),**[1, 2]**using projector augmented wave (PAW) pseudo potentials. The valence states set considered here, are Zn ($3d^{10}$ $4s^2$), Al ($3s^2$ $3p^1$), Cr ($3d^5$ $4s^1$), Ga ($4s^2$ $4p^1$), and O ($2s^2 2p^4$, 6 valence electrons). Perdew−Burke−Ernzerhof (PBE) functional under generalized gradient approximations (GGA) was used during geometry optimization process. **[3, 4]**

The kinetic energy cut off for plane wave basis has been fixed at 800 eV. Energy convergence of 10^{-6}eV has been chosen for self-consistent iteration. Brillouin zone sampling has been carried out by Γ-centered k-point mesh of 4 × 4 × 4 for 56 atom cell using Monkhorst and Pack scheme.**[5]**For electronic structure calculations, we have employed Heyd−Scuseria−Ernzerhof(HSE) hybrid density functional, which has been shown to reproduce experimental band gap for wide range of materials.**[6]**In HSE functional, the ion-core interaction is divided into short range (SR) and long range (LR) parts. The interaction part at short-range is described by both exact Hartree-Fock (HF) exchange with Perdew−Burke−Ernzerhof (PBE)

exchange, while the long-range part is only defined by PBE. The exchange-correlation energy (E_{XC}^{HSE}) is given by the expression below, **[7]**

$$E_{XC}^{HSE} = a\ E_X^{SR}(\mu) + (1-a)\ E_X^{PBE,\,SR}(\mu) + E_X^{PBE,\,LR}(\mu) + E_C^{PBE} \qquad (1)$$

Where $'\mu'$ is the screening parameter (0.2 $Å^{-1}$), and 'a' indicates mixing HF coefficient (25%). The figures for crystal structure have been generated using the graphical software, VESTA. **[8]**

S4. Rietveld refinement of powder XRD pattern

Powder XRD patterns were analysed further for determining lattice constants using FullProf software. The initialestimates of lattice parameters were taken from literature. Cation inversion was not considered in this fitting and all the systems and the quality of XRD data didn't permit to evaluate these parameters. The lattice constants determined and fit quality parameters are list in Table S1.

Table S1. Parameters from Rietveld refinement of powder XRD patterns

Sample $ZnGa_{2-x}Al_xO_4$	Lattice constant (a=b=c) (Å)	Unit cell volume ($Å^3$)	Fitting parameters
x=0.0	8.3272 (2)	577.42(3)	R_p: 5.76;R_{wp}: 7.37 ; R_{exp}: 3.91; Chi^2: 3.54
x=0.25	8.3233 (2)	576.62 (3)	R_p: 5.27;R_{wp}: 6.45; R_{exp}: 3.92; Chi^2: 2.70
x=0.5	8.2939 (4)	570.52(4)	R_p: 5.55;R_{wp}: 7.54; R_{exp}: 3.81; Chi^2: 3.91
x=1.0	8.2158 (4)	554.56(4)	R_p: 5.85; R_{wp}: 7.88; R_{exp}: 3.85; Chi^2: 4.19
x=1.5	8.1386 (3) 8.297 (2)*	539.08(4) 571.3 (2)*	R_p: 5.04 ; R_{wp}: 6.84; R_{exp}: 3.73; Chi^2: 3.36
x=2.0	8.0859 (2)	528.67 (2)	R_p: 5.60; R_{wp}: 7.53; R_{exp}: 3.92; Chi^2: 3.69

*8% $ZnGa_2O_4$ phase was present.

S5. Confocal microscopy

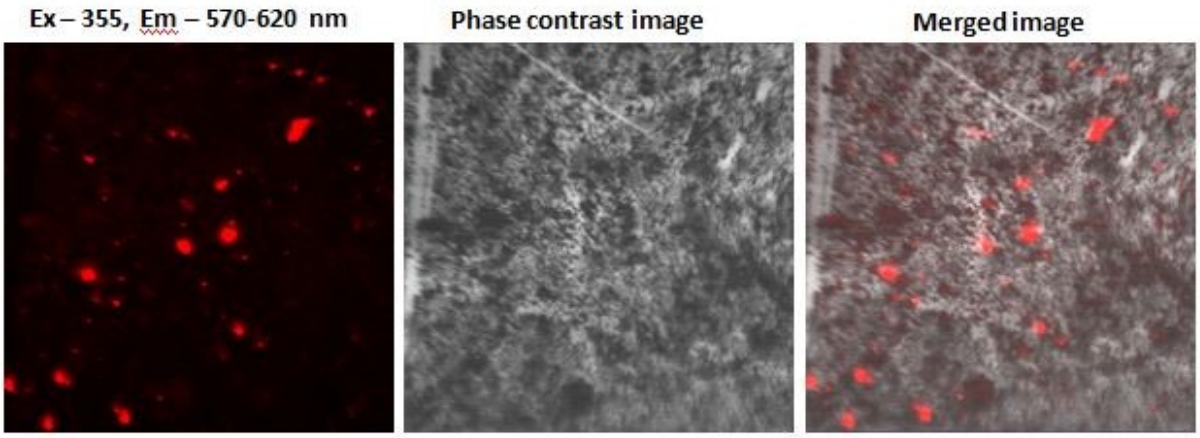

Figure S1: Correlation between particle size and red light emission as seen in correlation with fluorescence image and phase contrast image

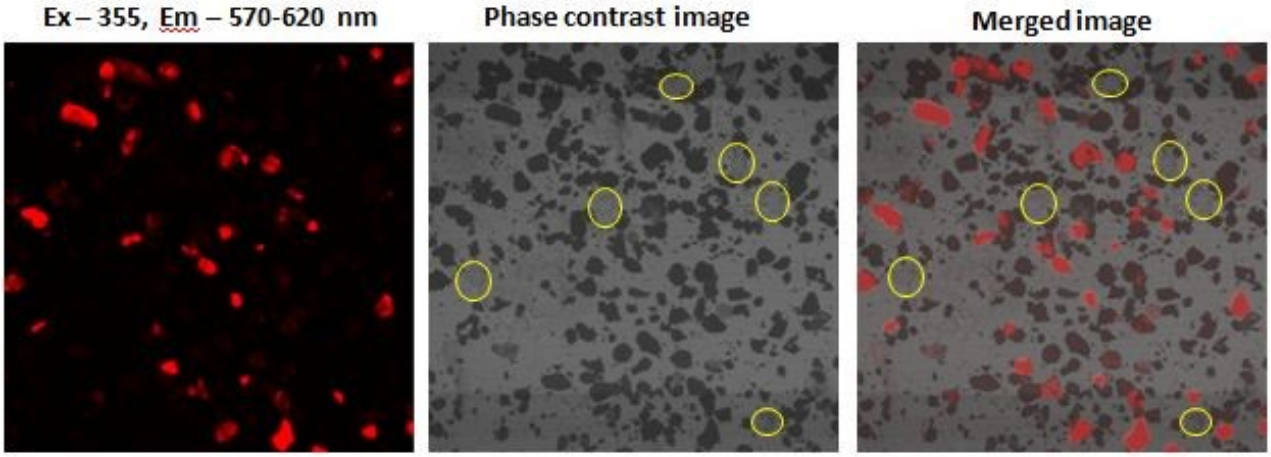

Figure S2: Fluorescence spectra of $ZnGa_{1.75}Al_{0.25}O_4:Cr^{3+}$incubated with human cells (osteosarcoma- U2OS) for 2husing confocal microscope along with phase contrast and merged image

S6. DFT results

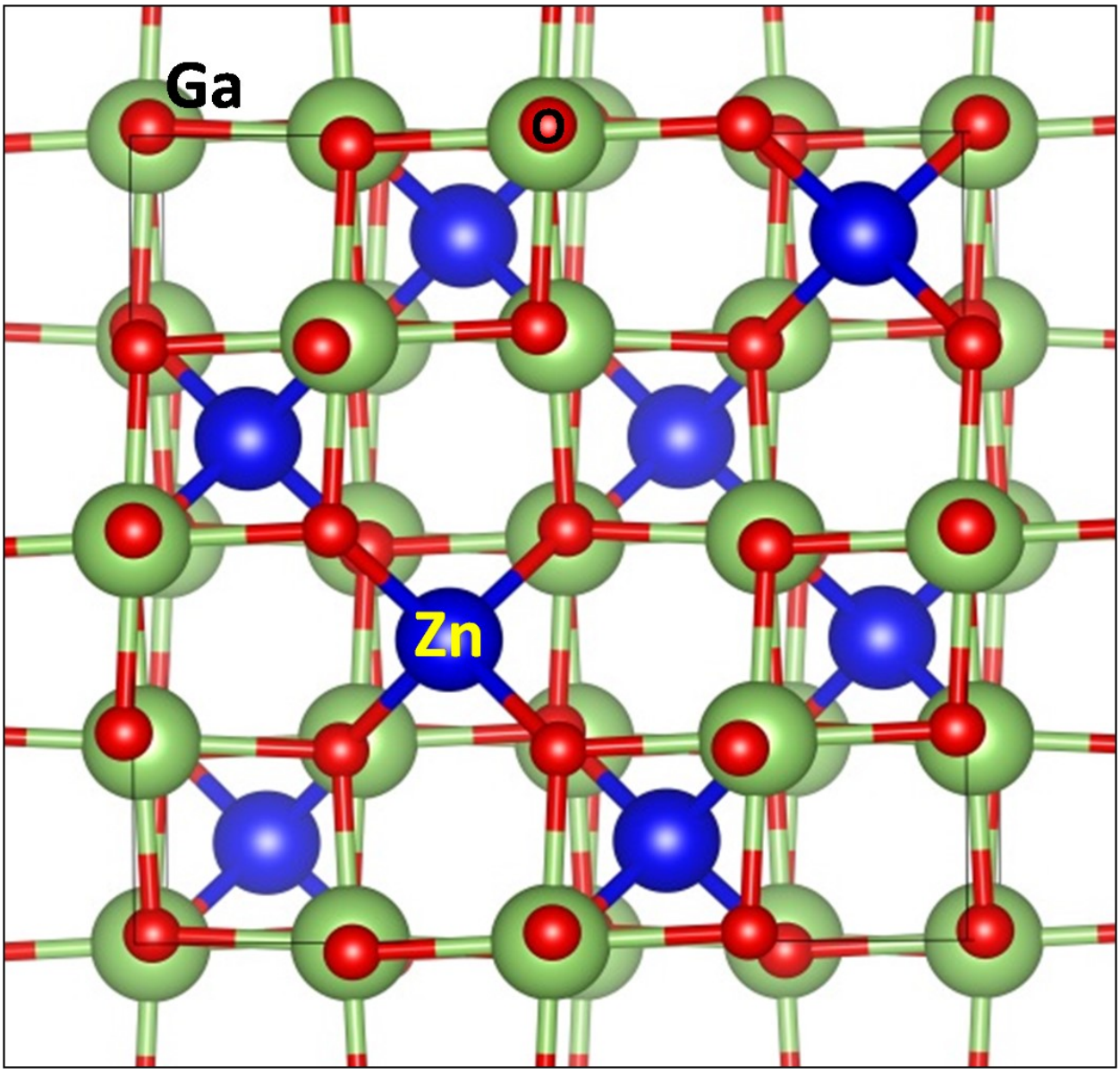

Figure S3: Crystal Structure of $ZnGa_2O_4$

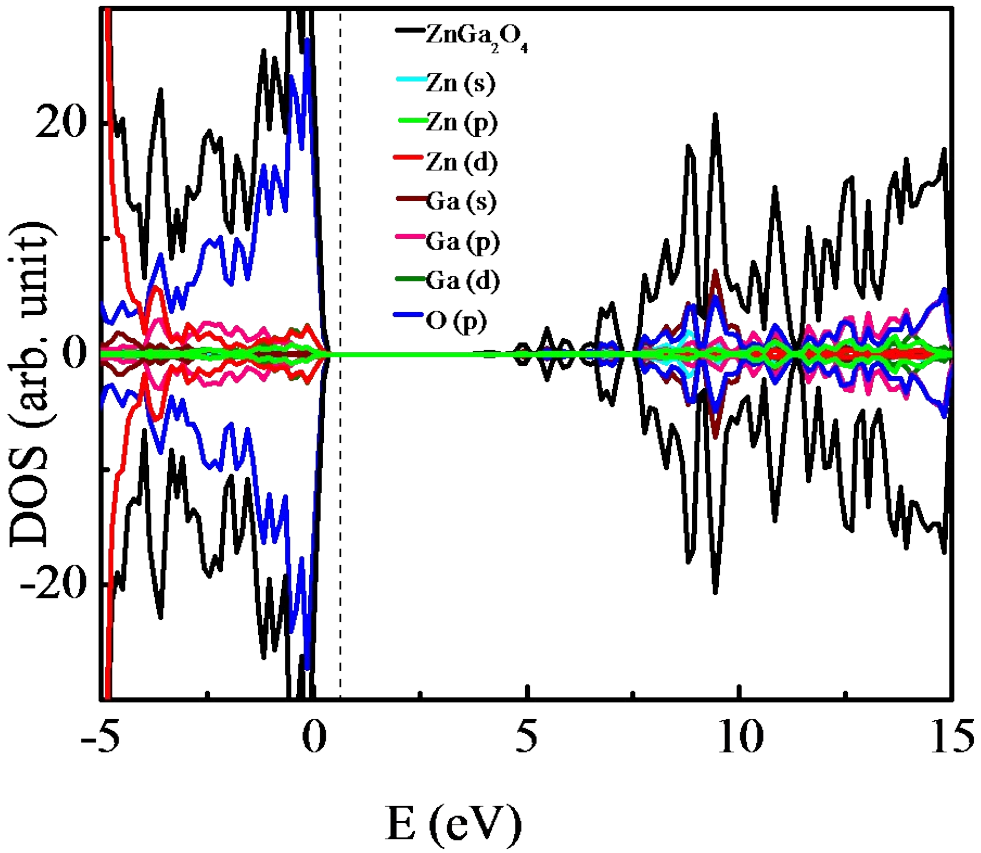

Figure S4: Density of states for $ZnGa_2O_4$. Vertical dashed line indicates the Fermi level.

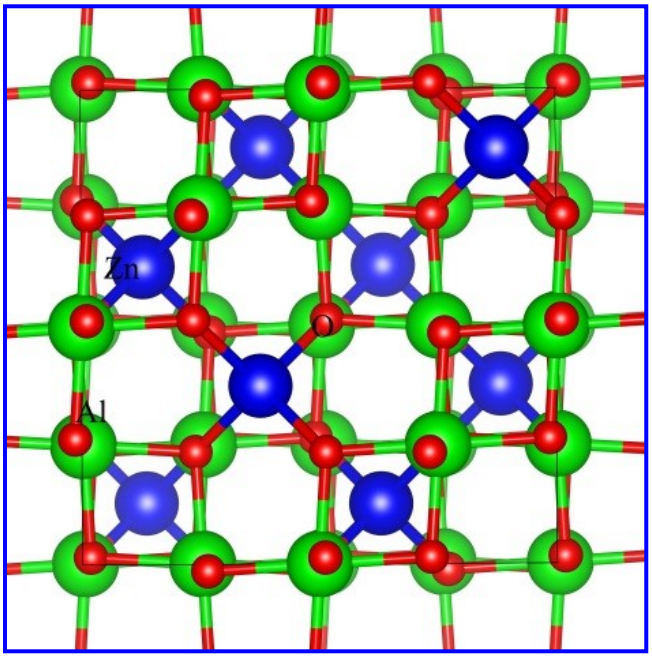

Figure S5: Crystal Structure of $ZnAl_2O_4$

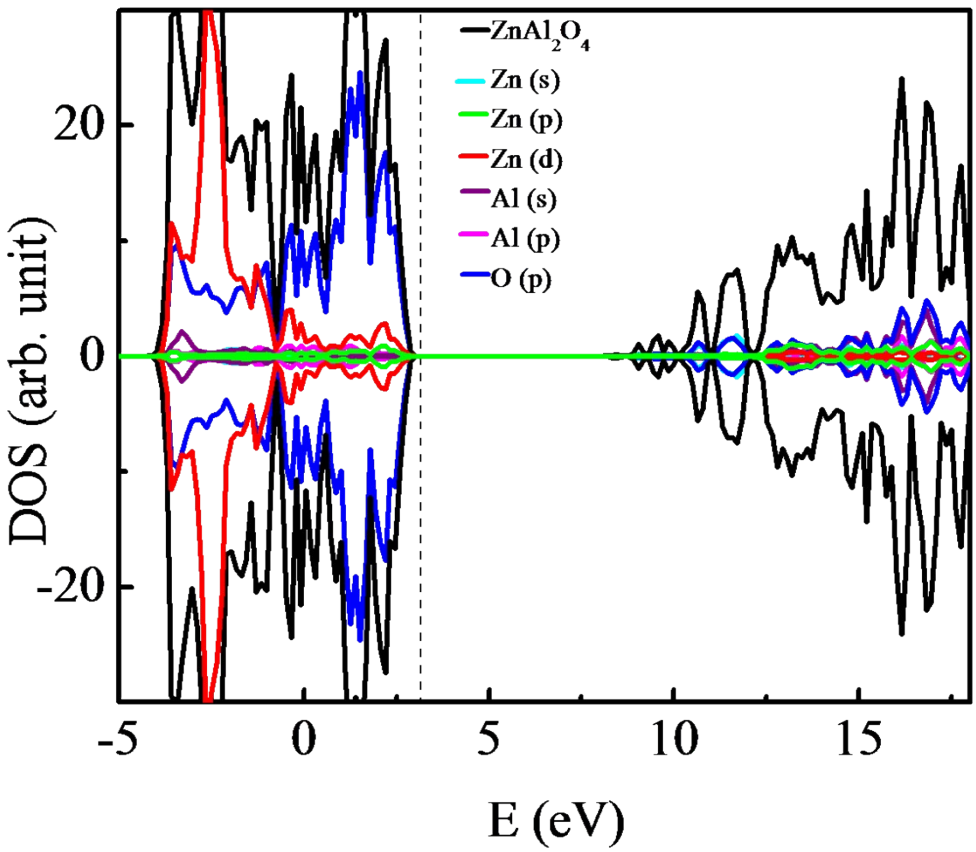

Figure S6: Density of states for $ZnAl_2O_4$. Vertical dashed line indicates the Fermi level.

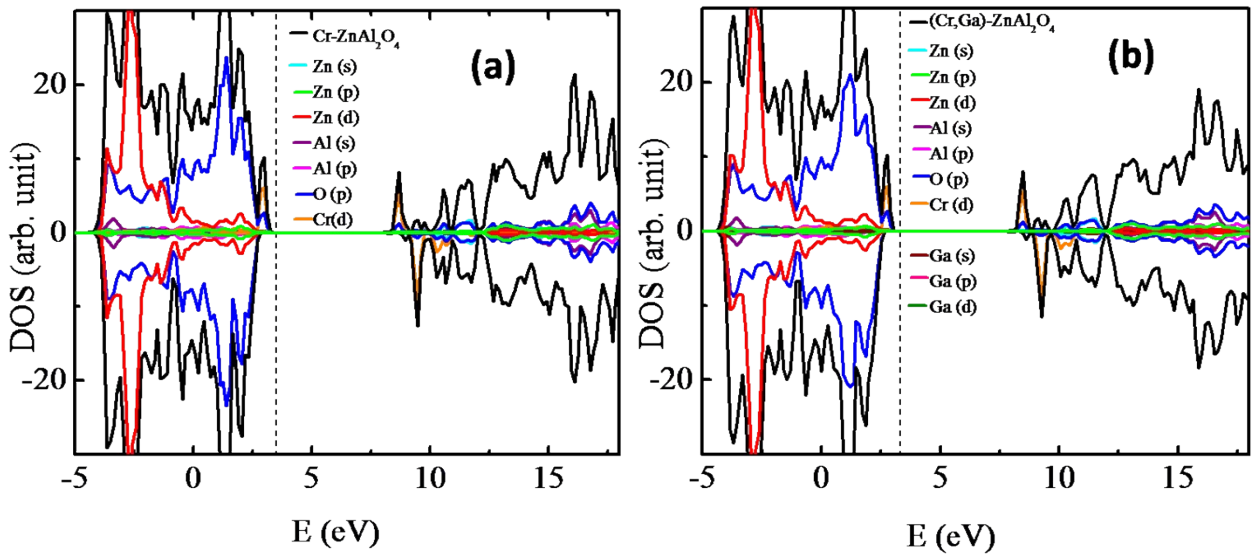

Figure S7: (a) Density of states for Cr-doped $ZnAl_2O_4$ and (b)(Cr, Ga)-codoped $ZnAl_2O_4$. Vertical dashed line indicates the Fermi level

References:

1. Kresse, G.; Joubert, D. From UltrasoftPseudopotentials to the Projector Augmented-Wave Method. Phys. Rev. B: Condens. Matter Mater. Phys. 1999, 59, 1758.
2. Blöchl, P. E. Projector Augmented-Wave Method. Phys. Rev. B: Condens. Matter Mater. Phys. 1994, 50, 17953.
3. Perdew, J. P.; Chevary, J. A.; Vosko, S. H.; Jackson, K. A.; Pederson, M. R.; Singh, D. J.; Fiolhais, C. Atoms, Molecules, Solids, and Surfaces: Applications of the Generalized Gradient Approximation for Exchange and Correlation. Phys. Rev. B: Condens. Matter Mater. Phys. 1992, 46, 6671.
4. Perdew, J. P.; Burke, K.; Ernzerhof, M. Generalized Gradient Approximation Made Simple. Phys. Rev. Lett. 1996, 77, 3865−3868.
5. Monkhorst, H. J.; Pack, J. D. Special Points for Brillouin-Zone Integrations. Phys. Rev. B 1976, 13, 5188
6. Paier, J.; Marsman, M.; Hummer, K.; Kresse, G.; Gerber, I. C.; Ángyán, J. G. Screened hybrid density functionals applied to solids. J. Chem. Phys. 2006, 124, No. 154709
7. Paier, J.; Marsman, M.; Hummer, K.; Kresse, G.; Gerber, I. C.; Ángyán, J. G. Screened hybrid density functionals applied to solids. J. Chem. Phys. 2006, 124, No. 154709
8. Momma, K.; Izumi, F. A Three-Dimensional Visualization System for Electronic and Structural Analysis. J. Appl. Crystallogr. 2008, 41, 653−658.